Stabilising high energy orbit oscillations by the utilisation of centrifugal effects for rotating-tyre-induced energy harvesting

Yunshun Zhang,[1,5,b)] Rencheng Zheng,[2,5,a)] Kimihiko Nakano,[3,5] and Matthew P. Cartmell[4,5]

[1] *Automobile Engineering Research Institute, Jiangsu University, Zhenjiang, 212013, China*

[2] *School of Automotive Engineering, Dalian University of Technology, Dalian, 116024, China*

[3] *Interfaculty Initiative in Information Studies, The University of Tokyo, Tokyo, 153-8505, Japan*

[4] *Mechanical and Aerospace Engineering, University of Strathclyde, Glasgow, G1 1XJ, Scotland, United Kingdom*

[5] *Institute of Industrial Science, The University of Tokyo, Tokyo, 153-8505, Japan*

Nonlinear energy harvesters are frequently considered in preference to linear devices because they can potentially overcome the narrow frequency bandwidth limitations inherent to linear variants; however, the possibility of variable harvesting efficiency is raised for the nonlinear case. This paper proposes a rotational energy harvester which may be fitted into an automobile tyre, with the advantage that it may broaden the rotating frequency bandwidth and simultaneously stabilise high-energy orbit oscillations. By consideration of the centrifugal effects due to rotation the overall restoring force will potentially be increased for a cantilever implemented within the harvester, and this manifests as an increase in its equivalent elastic stiffness. In addition this study reveals that the initial potential well barriers become as shallow as those for a bistable system. When the rotational frequency increases beyond an identifiable boundary frequency the system transforms into one with a potential barrier of a typical monostable system. On this basis the inter-well motion of the bistable system can provide sufficient kinetic energy so that the cantilever maintains its high-energy orbit oscillation for monostable hardening behaviour. Furthermore, in a vehicle drive experiment it has been shown that the effective rotating frequency bandwidth can be widened from 15 km/h – 25 km/h to 10 km/h – 40 km/h. In addition it is confirmed that the centrifugal effects can improve the harvester performance, producing a mean power of 61 μW at a driving speed of 40 km/h, and this is achieved by stabilising the high-energy orbit oscillations of the rotational harvester.

Given the generally narrow bandwidth of operating frequency for traditional linear systems it is natural to want to explore technologies that may broaden the bandwidth in order to convert optimally the energy in as much of the surrounding vibrational excitations into a useful electrical form as possible. Various principles have been already explored including resonant frequency tuning, the use of multi-frequency converter arrays, frequency-up conversion, and specific nonlinear approaches. As linear energy harvesters can only usually deliver power when the excitation frequency closely

a) Electronic mail: my_topzrc@yahoo.co.jp.

b) Electronic mail: zysgluck@ujs.edu.cn.

matches the natural frequency, several researchers have already proposed varying the position of the proof mass and the piezoelectric actuators structures that can be usefully applied within harvester structures in order to self-tune the natural frequency of such systems to increase the effectiveness of energy harvesting.[1,2] Arrays of harvester elements that can be set up to constitute multi-frequency systems comprising several beams or masses units, each one of them operating with different natural frequencies due to the designed-in characteristics of the components, can be useful for widening the operating frequency range.[3,4] Frequency-up conversion is adopted for amplification of the response of harvesters from low frequency ambient sources to the naturally higher operating frequencies of mechanical vibration harvesters.[5-7]

Many researchers have recently concentrated on nonlinear systems as a means of extending the coupling between the excitation and a harmonic oscillator to a wider bandwidth compared to the naturally narrower bandwidth of linear resonators.[8-12] The off-resonance approaches implemented in the design of such systems can introduce a nonlinear restoring force based on the use of magnetic or mechanical forces, without the need for natural frequency self-tuning.[13,14] Nonlinear energy harvesters can generally be classified into bistable[15-17] and monostable[18-20] variants, but in general the operational frequency bandwidth can be widened and the effectiveness of energy harvesting can be improved due to the existence of high energy orbit oscillation. Meanwhile, because of the co-existence of unstable and low-energy orbits it is necessary to stabilise the high-energy orbit motion by an appropriate adjustment of key system parameters,[21,22] or by the introduction of further kinetic energy,[23] to cope with a wider and variable frequency range for the environmental excitations to be harvested.

In most cases of real-world rotational environments in which harvestable amounts of vibrational energy can be found, the centrifugal acceleration generated in a proof mass can be more significant than the gravitational acceleration effect, particularly as the rotational frequency increases. Therefore, this paper focuses on the proposition that a nonlinear system with the addition of an active centrifugal force, can be investigated, both theoretically and experimentally within an actual vehicle tyre. Although passive self-tuning linear and pendulum energy harvesters have been adopted for harvesting rotational motion by utilising the effect of centrifugal force, there can be issues of maintaining commensurate relationships between the device's natural frequency and the external excitation frequency, and this can result in low energy harvesting efficiency over a wide frequency range.[24,25]

In this paper, principally because of the addition of centrifugal effects, the bistable state can be transformed into a monostable hardening form, and the high-energy orbit oscillation of the bistable system then supplies sufficient kinetic energy to stabilise the oscillation, shifting it to a monostable hardening characteristic, which can further broaden the operational frequency range, when run with a combination of high-energy orbit oscillations.

This manuscript was accepted by Appl. Phys. Lett. Click here to see the version of record.

Fig. 1 shows the proposed structure of a rotating energy harvester in a tyre, and it is seen to comprise two magnetic masses, each with the same polarity, and a rectangular cantilever beam with an attached piezoelectric film. Because of the repulsion effect between the magnetic masses the restoring force in the cantilever beam becomes inherently nonlinear and generates a bistable characteristic, but only if the distance between the two magnetic masses d is close enough. The harvester is radially positioned at the centre of rotation with a centrifugal distance l' between the centre of rotation and the barycentre of the magnetic proof mass. The rotation of the proof mass generates an additional tensile stress resulted from centrifugal acceleration of $\omega^2 l'$ in the centrifugal direction F_c which can be resolved into components f_c in the axial direction of the tip of the cantilever, and f_t in the tangential direction. Based on a preliminary theoretical analysis,[26] f_t can be used to tune the resultant linear stiffness of the harvester owing to the variable rotation frequency of ω. The dynamic equation of motion under additionally considering of centrifugal acceleration is re-governed as follows,

$$M\ddot{u} + c\dot{u} + \left(k - \frac{F_m}{d} + \frac{3M\omega^2 l'}{2L} \right) u + bu^3 = G\sin\left(\omega t + \eta_0\right). \tag{1}$$

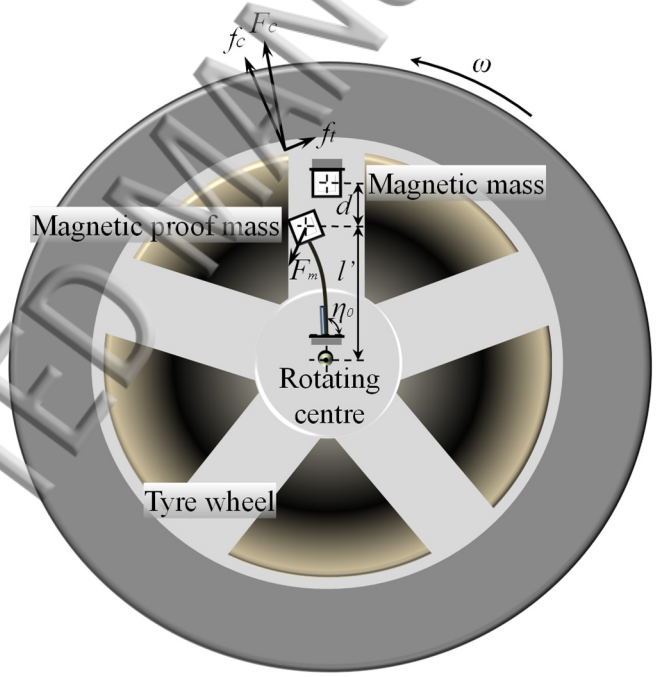

FIG. 1. Schematic of a rotating tyre energy harvester model.

In Eq. (1), M is the magnetic proof mass, u is the vibrational amplitude of the cantilever beam at the tip position, and c is the viscous damping coefficient including both mechanical and electrical constituent parts. In addition, k represents the lateral stiffness of the cantilever beam, L defines the dimensional length of the beam, and b is the nonlinear coefficient which results from the repulsive effect between the two adjacent magnets. Due to the much higher acceleration of centrifugal force than

This manuscript was accepted by Appl. Phys. Lett. Click here to see the version of record.

gravity with the increasing rotating frequency, and the tiny deflection angular at the tip of cantilever, the tangentially resolved component involving the deflection angular of gravity force can be neglected, and mainly focus on its effect of acting as the harmonic excitation of input exploited in this research. The harmonic excitation is generated from the gravity effect on the proof mass G combined with the dynamics of rotation at a frequency of ω, and it should also be noted that η_0 is the initial angle between the central axis of the beam and the horizontal direction. The polynomial representation of the equivalent linear stiffness leads to $\left(k-F_m/d+3M\omega^2 l'/2L\right)$ from the coefficient of the third term, where F_m and d are the repulsive magnetic fore and distance between magnets. The expression of potential energy U_0' after considering the centrifugal effect is obtained based on the coefficients of the third and fourth terms of Eq. (1),

$$U_0'(u,t)=\frac{1}{2}\left(k-\frac{F_m}{d}+\frac{3M\omega^2 l'}{2L}\right)u^2+\frac{1}{4}bu^4, \tag{2}$$

when in the initial bistable state the coefficient of $\left(k-F_m/d\right)$ is negative, therefore $\left(k-F_m/d\right)=-a$, (a>0). However, if the centrifugal effect defined by $\left(3M\omega^2 l'/2L\right)$ is added into the stiffness term for the cantilever beam, the coefficient of the third term tends to change from its initially negative value into a positive value.

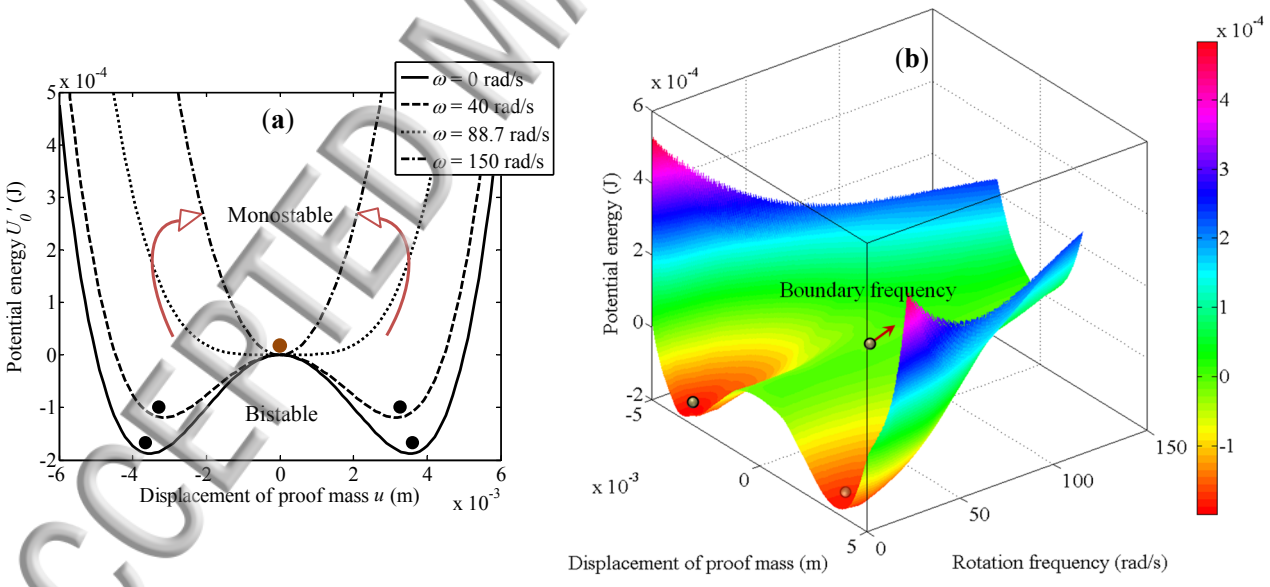

FIG. 2. (a) Potential energy against the displacement of proof mass; (b) variation of the potential energy as a function of rotation frequency and displacement of proof mass, under the same parameter conditions: a = 60 (N/m), b = 4.8 × 10^6 (N/m^3), m = 8 g, c = 0.08 (N/m/s), k = 152.7 (N/m), and L = 4.2 cm.

This manuscript was accepted by Appl. Phys. Lett. Click here to see the version of record.

In practice, when the system starts to rotate it can transform from a bistable characteristic into a monostable response at some chosen boundary frequency. The expression for the boundary frequency ω_b can be obtained by assuming that the polynomial representing the equivalent linear stiffness is equal to zero, hence,

$$\omega_b = \sqrt{\frac{2L\left(\frac{F_m}{d} - k\right)}{3ml'}}. \tag{3}$$

As shown in Fig. 2, in the initial rotation frequency of 0 rad/s, the term of $\left(k - F_m/d\right)$ keeps the negative characteristic, which shows the bistable state with two deep potential barriers. As the speed increases by a rotation frequency of 40 rad/s, the system remains the bistable state with two shallower potential barriers, and when ω exceeds the defined boundary frequency of 88.7 rad/s to a higher frequency of 150 rad/s, the system alters from its originally bistable state to a monostable state. The frequency-amplitude response equation for the bistable system can be obtained by applying the harmonic balance method, leading to,

$$\frac{9}{16}b^2U^6 - \frac{3}{2}b\left(m\omega^2 + a\right)U^4 + \left[\left(m\omega^2 + \frac{F_m}{d} - \frac{3m\omega^2 l'}{2L} - k\right)^2 + c^2\omega^2\right]U^2 - G^2 = 0, \tag{4}$$

where U is the velocity amplitude response of the cantilever beam at the tip position. Solving the frequency-amplitude response equation of the transformed monostable hardening system for physically realistic solutions yields a jump-down frequency expression for the monostable state, as given by,

$$\gamma' = \sqrt{\frac{1}{2m}\left(\sqrt{\left(\frac{2aL - 3m\omega^2 l'}{2L}\right)^2 + \frac{3mbG^2}{c^2}}\right) + \frac{2aL - 3m\omega^2 l'}{4mL}}. \tag{5}$$

In order to validate experimentally the effectiveness of the centrifugal effect on stabilising the high-energy orbit and therefore further improving the operational bandwidth, a practical maximum driving speed of 40 km/h was assumed, and this corresponded to a rotation frequency of 38.2 rad/s. Therefore the key task is that of optimising the appropriate centrifugal distance, with a compatible softening stiffness of the cantilever beam, to enable a useful vehicle drive experiment. The numerical investigations were carried out for the following parameter conditions: a = 10 (N/m), $b = 2 \times 10^4$ (N/m^3), m = 8 g, c = 0.08 (N/m/s), k = 30 (N/m), and L = 4.5 cm. The results shown in Fig. 3 using Eq. (4) for the centrifugal condition of 0 cm, which reduces the centrifugal force to zero show that the high energy orbit motion can be continued until the frequency reaches 29.1 rad/s and displays bistable behaviour.

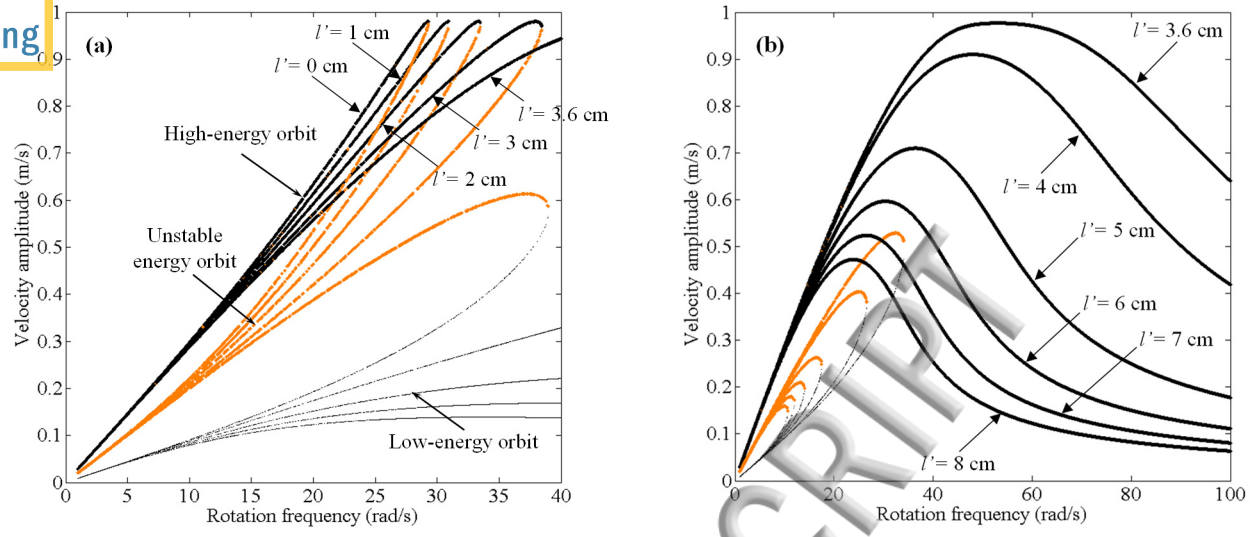

FIG. 3. Frequency-amplitude response under different centrifugal distances: (a) 0 cm-3.6 cm; (b) 3.6 cm-8 cm.

By increasing the distance to 1 cm the high-energy oscillation can be stabilised for a slightly wider bandwidth of 30.9 rad/s because of the shallower depth of the potential well when the centrifugal effect is added in. The transformational effect from bistability to monostability occurs at a boundary frequency of 60.2 rad/s due to Eq. (3), and this makes the system jump down to the low-energy orbit after a frequency of 30.9 rad/s.

Increasing the distance further to 3 cm shows that the boundary frequency is reduced to 34.6 rad/s. It can be interpreted from Fig. 3(a) that the high-energy orbit oscillation, below a frequency of 34.6 rad/s, contains sufficient kinetic energy to stabilise the oscillation until the turn down point at 38.8 rad/s. When the centrifugal distance is set to 3.6 cm the high-energy orbit oscillation can invariably be maintained within a frequency of 40 rad/s, and the boundary frequency defining the transformation from bistability to monostability, is found to be 31.6 rad/s, again on the basis of applying Eq. (3).

Fig. 3(b) demonstrates that the frequency-amplitude response within a rotation frequency domain of zero to 100 rad/s, while the centrifugal distances are all set to exceed 3.6 cm. As the distance increases the boundary frequency gradually drops down, which results in a narrowing of the response frequency region for bistability, and so the effect of bistability on the velocity response of the cantilever becomes weaker. In these cases it is more difficult to obtain sufficient initial kinetic energy to stimulate a stabilised monostable high-energy orbit oscillation, and the velocity response of the cantilever gradually falls away.

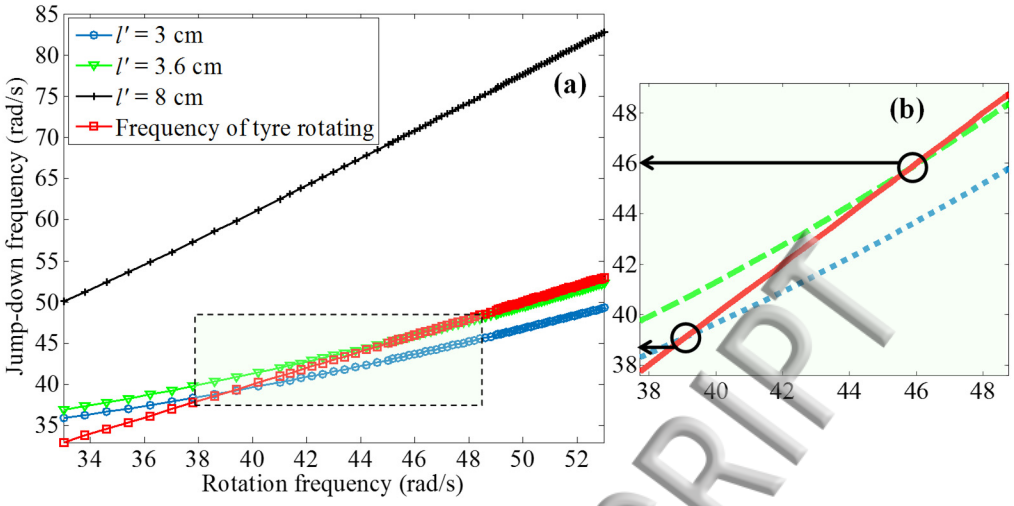

FIG. 4. (a) Variation of jump down frequency with increasing rotation frequency; (b) a partially enlarged view.

Eq. (5) is used to calculate a curve for the jump-down frequency as a function of the rotation frequency, and this is characteristic is given in Fig. (4). The blue line shows that the rotation frequency can keep up with the jump down frequency at 38.8 rad/s, and this enables the high energy orbit to be sustained over a broader bandwidth above 34.6 rad/s. The green line shows that the, rotation frequency can keep up with the jump down frequency until 46 rad/s, and this can hypothetically be regarded as the resonant frequency of the linear system. Exceeding a distance of 3.6 cm means that the increasing rate of the centrifugal force is greater than that of the tyre rotation so the rotation frequency can never match the jump down frequency of the monostable system.

Fig. 5 summaries the derived simulation result by comparison of the mean velocity amplitude at different distances, and it can be revealed that with an increase in the centrifugal distance the efficient harvesting bandwidth is further enlarged, and the widest bandwidth is found to be for 3.6 cm, this being approximately consistent with the result for the frequency-amplitude curve shown in Fig. 3(a) (the corresponding real-time velocity responses under distances of 0cm, 3.6 cm and 7 cm see supplementary material, S1, S2 and S3).

Fig. 6 demonstrates that an actual vehicle experiment (the description of apparatus see supplementary material) was undertaken to corroborate the positive harvesting effect of the centrifugal force by measuring the centrifugal distance at 0 cm, 3.6 cm and 7 cm, respectively, from the centre of rotation of the tyre with the same configuration as given in Fig. 1. As shown in Figs. 7(a), 7(b) and 7(c), a simulation of the root mean square (RMS) power was derived by modelling the equivalent electric circuit of the piezoelectric transducer, and relating this to its displacement characteristic (see supplementary material). It was found that the simulation results agreed well with the experimental results for the three centrifugal distances, using a load resistor of 150 kΩ.

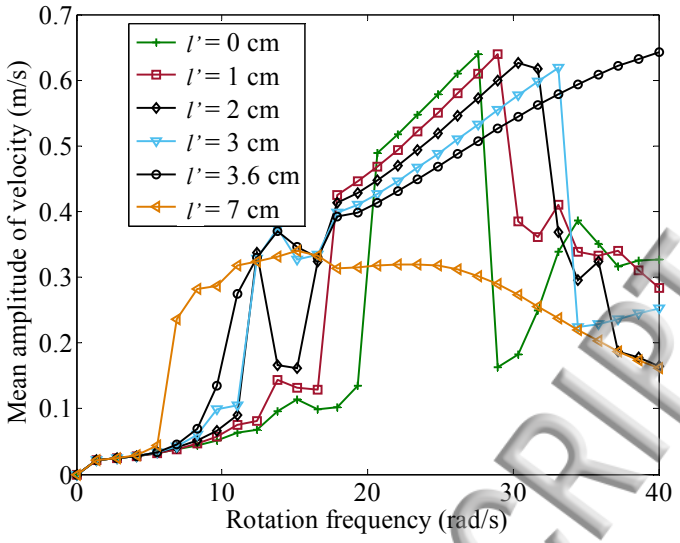

FIG. 5. Simulation result for the validation of efficient bandwidth under different rotating centrifugal distances.

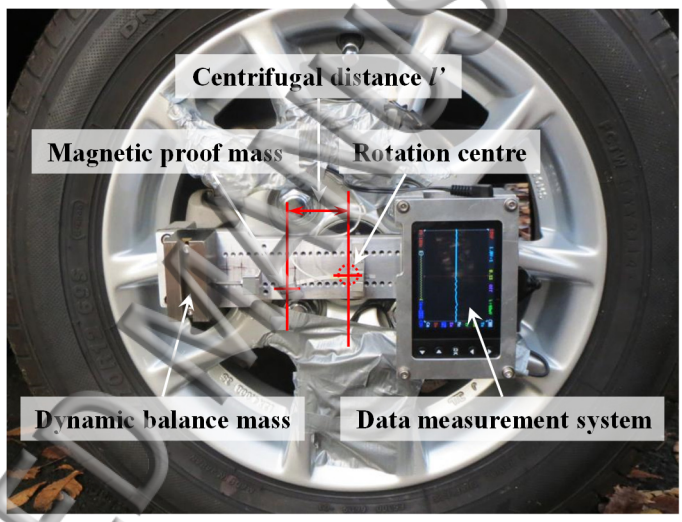

FIG. 6. Apparatus for the actual-vehicle experiment under different centrifugal distances: $l' = 0$ cm; $l' = 3.6$ cm; $l' = 7$ cm.

By comparing the experimental results as shown in Fig. 7 it can be concluded that the operating speed range for the vehicle can be extended to 10 km/h – 40 km/h for a centrifugal distance of 3.6 cm, and this is broader than the speed range of 15 km/h – 25 km/h when the centrifugal distance is zero. The maximum power generation can reach 0.24 mW with a mean power of 61 μW, and the corresponding maximum voltage is 6 V with a mean voltage of 2.46 V at a driving speed of 40 km/h.

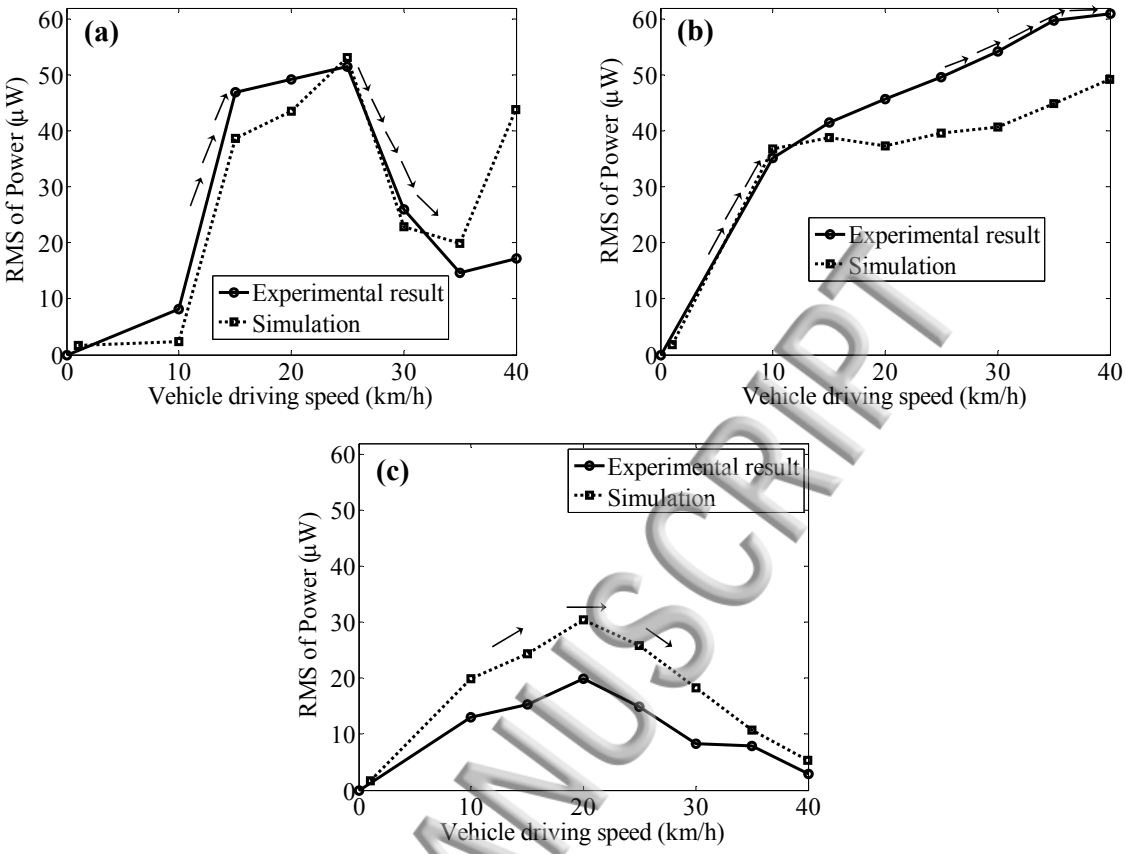

FIG. 7. Comparative results under different centrifugal distances: (a) l' = 0 cm; (b) l' = 3.6 cm; (c) l' = 7 cm.

In conclusion, this paper suggests that there are clear advantages in considering the centrifugal effect in a rotating tyre energy harvesting, and that it can outperform a simple bistable or monostable harvester in which the centrifugal effect is absent. The proposed approach can therefore be potentially more efficient in that it clearly broadens the operational bandwidth of the harvester and simultaneously stabilises the high-energy orbit oscillations thereby improving the overall effectiveness of a rotational energy harvester.

Supplementary Material

See supplementary material for the simulation results of real-time velocity responses under centrifugal distances of 0cm, 3.6 cm and 7 cm, concrete description of the apparatus for actual-vehicle experiment and modelling analysis of equivalent electric circuit of piezoelectric transducer.

[1]L. M. Miller, P. Pillatsch, E. Halvorsen, P. K. Wright, E. M. Yeatman, and A. S. Holmes, J. Sound Vib. **332**(26), 7142 (2013).

[2]C. Eichhorn, F. Goldschmidtboeing, Y. Porro, and P. Woias, in *Power MEMS* (2009), pp. 45–48.

[3]S. M. Shahruz, J. Sound Vib. **292**(3), 987 (2006).

[4]J. Chen, D. Chen, T. Yuan, and X. Chen, Appl. Phys. Lett. **100**(21), 213509 (2012).

[5]S. M. Jung and K. S. Yun, Appl. Phys. Lett. **96**(11), 111906 (2010).

[6]P. Pillatsch, E. M. Yeatman, and A. S. Holmes, Sensor. Actuat. A-Phys. **206**, 178 (2014).

[7]H. Fu and E. M. Yeatman, Energy **125**, 152 (2017).

[8]F. Cottone, H. Vocca, and L. Gammaitoni, Phys. Rev. Lett. **102**(8), 080601 (2009).

[9]B. P. Mann and N. D. Sims, J. Sound Vib. **319**(1), 515 (2009).

[10]D. A. Barton, S. G. Burrow, and L. R. Clare, J. Vib. Acoust. **132**(2), 021009 (2010).

[11]S. C. Stanton, C. C. McGehee, and B. P. Mann, Physica D **239**(10), 640 (2010).

[12]M. F. Daqaq, R. Masana, A. Erturk, and D. D. Quinn, Appl. Mech. Rev. **66**(4), 040801 (2014).

[13]L. Gammaitoni, I. Neri, and H. Vocca, Appl. Phys. Lett. **94**(16), 164102 (2009).

[14]R. Masana and M. F. Daqaq, J. Vib. Acoust. **133**(1), 011007 (2011).

[15]A. Erturk, J. Hoffmann, and D. J. Inman, Appl. Phys. Lett. **94**(25), 254102 (2009).

[16]A. Erturk and D. J. Inman, J. Sound Vib. **330**(10), 2339 (2011).

[17]R. L. Harne and K. W. Wang, Smart Mater. Struct. **22**(2), 023001 (2013).

[18]B. Marinkovic and H. Koser, Appl. Phys. Lett. **94**(10), 103505 (2009).

[19]P. L. Green, K. Worden, K. Atallah, and N. D. Sims, J. Sound Vib. **331**(20), 4504 (2012).

[20]E. Halvorsen, Phys. Rev. E **87**(4), 042129 (2013).

[21]R. Ramlan, M. J. Brennan, B. R. Mace, and I. Kovacic, Nonlinear Dynam. **59**(4), 545 (2010).

[22]D. Su, R. Zheng, K. Nakano, and M. P. Cartmell, P. I. Mech. Eng., C-J. Mec. **230**(12), 2003 (2016).

[23]S. Zhou, J. Cao, D. J. Inman, S. Liu, W. Wang, and J. Lin, Appl. Phys. Lett. **106**(9), 093901 (2015).

[24]L. Gu and C. Livermore, Appl. Phys. Lett. **97**(8), 081904 (2010).

[25]L. Gu and C. Livermore, Smart Mater. Struct. **21**(1), 015002 (2010).

[26]Y. Zhang, K. Nakano, R. Zheng, and M. P. Cartmell, J. Phys.: Conf. Ser. **744**(1), 012079 (2016).